

AGN Feedback Signatures in UV Emission

K. Rubinur [†] 

Institute of Theoretical Astrophysics, University of Oslo, P.O. Box 1029, Blindern, 0315 Oslo, Norway;
rubinur.khatun@astro.uio.no

Abstract: Supermassive black holes (SMBH) are believed to influence galaxy evolution through AGN (active galactic nuclei) feedback. Galaxy mergers are key processes of galaxy formation that lead to AGN activity and star formation. The relative contribution of AGN feedback and mergers to star formation is not yet well understood. In radio-loud objects, AGN outflows are dominated by large jets. However, in radio-quiet objects, outflows are more complex and involve jet, wind, and radiation. In this review, we discuss the signatures of AGN feedback through the alignment of radio and UV emissions. Current research on AGN feedback is discussed, along with a few examples of studies such as the galaxy merger system MRK 212, the radio-quiet AGN NGC 2639, and the radio-loud system Centaurus A. Multi-frequency observations of MRK 212 indicate the presence of dual AGN, as well as feedback-induced star-forming UV clumps. The fourth episode of AGN activity was detected in radio observations of the Seyfert galaxy NGC 2639, which also showed a central cavity of 6 kpc radius in CO and UV maps. This indicates that multi-epoch jets of radio-quiet AGN can blow out cold molecular gas, which can further reduce star formation in the center of the galaxies. Recent UV observations of Cen A have revealed two sets of stellar population in the northern star-forming region, which may have two different origins. Recent studies have shown that there is evidence that both positive and negative feedback can be present in galaxies at different scales and times. High-resolution, multi-band observations of large samples of different types of AGN and their host galaxies are important for understanding the two types of AGN feedback and their effect on the host galaxies. Future instruments like INSIST and UVEX will be able to help achieve some of these goals.

Keywords: galaxies; active; AGN feedback; Seyfert; galaxy merger; UV continuum; radio continuum emission



Citation: Rubinur, K. AGN Feedback Signatures in UV Emission. *Galaxies* **2024**, *12*, 15. <https://doi.org/10.3390/galaxies12020015>

Academic Editor: Fulai Guo

Received: 29 February 2024

Revised: 31 March 2024

Accepted: 2 April 2024

Published: 4 April 2024



Copyright: © 2024 by the author. Licensee MDPI, Basel, Switzerland. This article is an open access article distributed under the terms and conditions of the Creative Commons Attribution (CC BY) license (<https://creativecommons.org/licenses/by/4.0/>).

1. Introduction

From an observational perspective, two important findings in extra-galactic astronomy are that (i) the star-formation density and AGN activity peak around redshift 2–3, which is known as the cosmic noon [1]; (ii) the mass of the central super-massive black holes correlates with galaxy properties like the SMBH mass-bulge velocity dispersion ($M-\sigma_*$) relation [2–4]. We still do not fully understand the reason for these correlations. AGN are believed to expel energy through jets, wind, or radiation [5]. These processes can blow out star-forming material and hence decrease the star-formation rate (SFR) in the galaxy, known as negative feedback. On the other hand, these outflows can also compress the star-forming material, making this an ideal scenario for star-formation causing positive feedback. Hence, to understand galaxy evolution, estimation of the effect of AGN feedback is important [6–9].

Most galaxy formation models require negative feedback to produce the present day's quenched massive galaxies. This ejects interstellar medium (ISM) gas and prevents the circumgalactic material gas from cooling and becoming accreted in the galaxies. This process helps to regulate the size and density of galaxies and produces the observed bimodality in galaxy colors. In the past two decades, theoretical models and simulations have included AGN feedback to improve galaxy formation and evolution [10–15]. The constraints provided by observations are important to improve theoretical models. The

observations of negative AGN feedback come from X-ray and radio studies of galaxy clusters. X-ray cavities and hot shock gas fronts are detected in these clusters, which coincide with the radio lobes. These studies suggest that a radio jet powers the surrounding medium and hence suppresses the gas cooling [16,17]. These studies suggest that even radio jets in weak AGN can be mechanically powerful. Hence, the effect of such radio jets can also be important in isolated galaxies [18,19]. However, in radio-quiet AGN (which is the majority of the galaxy population), the origin of radio emission is still not settled. Hence, the AGN outflows (jet, wind, radiation) are complex and the relative contribution from each component is still not understood [20–23].

Along with negative feedback, in the past decade, there have been detections of positive feedback in galaxies with evidence of jet-induced star formation [24,25]. Earlier studies of AGN feedback signatures were mostly based on ionized gas, which is mostly observed as long-slit spectroscopy (emission or absorption) [26]. There has been growing evidence of AGN feedback signatures (both positive and negative) in galaxies [27–33].

A few well-studied AGN outflows in radio-quiet AGN include MRK 231 [34], IC 5063 [35], NGC 1068 [32], etc. MRK 231 is the nearest quasar and shows wind-driven outflows. It has nuclear ultra-fast outflows (UFO) detected in X-ray, sub-kpc HII outflows, as well as kpc-scale molecular outflows [27,36–38]. These outflows show a wide angle and the radio jet in MRK 231 does not seem to drive the outflows [9]. Disturbed molecular gas and high excitation compared to the disk were detected along the radio jet in IC 5063 [39]. The spatial coincidence of the radio jet and outflow supports the radio jet being the dominant mechanism [40,41]. The galaxy merger, IRAS F23128-5919 hosts an obscured AGN. A multi-wavelength diagnostic showed star formation within the outflowing material [42]. Gallagher et al. [43] compiled a sample from MaNGA data and identified outflows in a sub-sample of 37 galaxies where 1/3rd of those showed signatures of star formation within the outflowing gas. The SFR ranged from 0.1 to $1 \text{ M}_{\odot} \text{ yr}^{-1}$, which could contribute to 5–30% of the total SFR in the galaxy. Recent observations, as well as simulations, suggest that both negative and positive feedback can work together and can be observed in some galaxies [44,45].

The alignment of non-thermal radio emission and UV emission also suggests jet-induced star formation [46,47]. UV emission arises from massive O-, B-, and A-type stars and hence traces star-formation within the age range of 10^6 to 10^8 yr [48,49]. Recently, Tamhane et al. [45] explored jet-ISM interaction in the central elliptical galaxy of the Abell 1975 cluster using multi-frequency observations. They concluded that radio jets that heat the gas on a large scale and over a large timescale can also trigger star formation through positive feedback over a shorter time scale. Duggal et al. [50] studied a sample of seven powerful compact steep spectrum (CSS) sources that have sub-galactic scale jets with a projected size of 1–20 kpc. UV continuum emission was detected in six sources. The UV emission showed alignment with the radio jets in five of those sources.

In this review, we discuss a few recent studies of possible AGN feedback signatures found in UV bands in different types of galaxy systems. These studies are mostly from UVIT [51] and GALEX [52]. UVIT is one of the five payloads onboard India's first astronomical satellite AstroSat [51]. The expected spatial resolution of UVIT is $\sim 1.2''$ to $\sim 1.5''$, while GALEX has $5''$. Both telescopes have FUV and NUV filters.

2. Galaxy Merger and Feedback

It is believed that blue star-forming galaxies move to red quiescent galaxies in the galaxy main sequence [53–56]. There are several processes through which the star-formation quenching happens, like AGN feedback [5,10,57–59], galaxy mergers [60–62], and environment effects such as ram-pressure stripping [63]. Our current understanding of galaxy formation is that galaxies grow through mergers [61,64]. The non-axisymmetric gravitational forces change the potential of the galaxies [65]. Simulations have found that mergers lead to gas inflow towards the nuclei as well as on the disk, hence increasing AGN activity and star formation [66]. Several studies have tried to understand the effect of mergers on star formation and AGN activity, as well as on galaxy evolution [67–69]. However, this is a complex process

to understand. (i) Merger-induced star-burst and AGN activity consume gas, (ii) they also blow out the gas through negative feedback, and (iii) AGN contributes to star-formation (positive feedback) during the merger in some galaxies like ultra-luminous infrared galaxies (ULIRGs) (e.g., [70]). So, galaxy mergers and AGN may work together [71,72]. However, the contribution of each mechanism is not well understood.

A sample of dual-nuclei galaxies was investigated with UVIT [73,74]. The motivation for this work was to understand star formation, as well as to look for any signatures of feedback. This pilot study had a sample of 10 galaxies where the nuclei are separate ≤ 11 kpc. It included four galaxies with confirmed AGN and the remaining six galaxies had star-forming nuclei. However, the nature of the star-forming nuclei came mostly from optical spectroscopy and a Baldwin, Phillips, and Terlevich (BPT) diagram [75]. It was recently found that many of the star-forming galaxies from the BPT diagram show AGN nuclei in X-ray or IR analysis [76,77]. Here, an investigation of one of the sample galaxies, MRK 212 with multi-wavelength data revealed interesting results on the nature of nuclei and star formation [73].

Galaxy Merger System: MRK 212

MRK 212 (Figure 1A) is a pinwheel galaxy (UGC 07593 NED02: S1) in an ongoing merger system with its companion (UGC 07593 NED01: S2) at redshift 0.022893. The SDSS image shows that the nuclei projected separation is 11.8 arcsec (~ 5.6 kpc). Both nuclei show radio emission in the 1.4 GHz Faint Images of the Radio Sky at Twenty cm image (<http://www.cv.nrao.edu/first/>), making it a good candidate for being DAGN (dual AGN). DAGN are close pairs of AGN, which is also an expected output of galaxy mergers where both the parent galaxies host central SMBH [78–83]. The coalescence of the pair of SMBH will generate gravitational waves that are of great interest for future astronomy [84]. On the other hand, the pair of AGN at different separations can help us to understand the evolution of SMBH, as well as the galaxy [83]. This requires very high-resolution multi-waveband observations to detect DAGN and there are still only a handful of detections. However, the number has started to increase in the past few years [80–82,85–88]. For MRK 212, the SDSS has only one spectrum assigned to S2 that is star-forming in nature.

The 8.5 GHz image (Figure 1B; [73]) revealed two radio structures at a separation of ~ 6 kpc, where S1 shows an unresolved structure with some extension in the north–south direction and S2 shows a double radio structure (A, B) of size ~ 2 Kpc, which is $1''$ offset from the optical nuclei (C). The Ku-band 15 GHz data showed a resolved extended structure associated with S1, while a compact core was associated with S2 (C) (Figure 1B). The 1.4 GHz upgraded Giant Metrewave Radio Telescope (uGMRT) (<http://www.gmrt.ncra.tifr.res.in/>) image shows two unresolved structures associated with S1 and S2. The optical spectra of both nuclei were obtained from the Himalayan Chandra Telescope (HCT; [89]). A deep 15 ksec UVIT image detected several UV-bright clumps (Figure 1C; [73]).

The double-lobe structure of S1 of size 750 pc at 15 GHz and a spectral index value of -0.81 ± 0.10 resembles a compact symmetric object [90]. However, the 1.4 GHz radio power ($\sim 10^{21}$ W Hz $^{-1}$) is lower than the compact spectrum object (CSO: [90]) and overlaps with the low-power AGN. The total radio power was compared with the average power of an individual supernova (2×10^{20} W Hz $^{-1}$) [91]. While a number of SNe could produce the observed radio luminosity, it is unrealistic to show a double structure around the nuclei. Rubinur et al. [73] concluded that the radio source associated with S1 is a CSO-like weak AGN. The compact core detected at the centre of S2 has a radio luminosity of $\sim 10^{21}$ W Hz $^{-1}$. This core is not detected at lower frequency images, and the detection at the highest observed frequency suggests that an inverted spectrum supports the synchrotron self-absorbed emission from the base of an unresolved jet. The HCT spectra put S1 and S2 in the composite region of the BPT diagram. From the fitted SDSS spectrum of S2, Hernández-Ibarra et al. [92] also classified it as an AGN. Based on the detection of the compact radio core, as well as optical spectra, Rubinur et al. [73] concluded that S2 is a weak AGN, hence confirming the dual AGN in MRK 212.

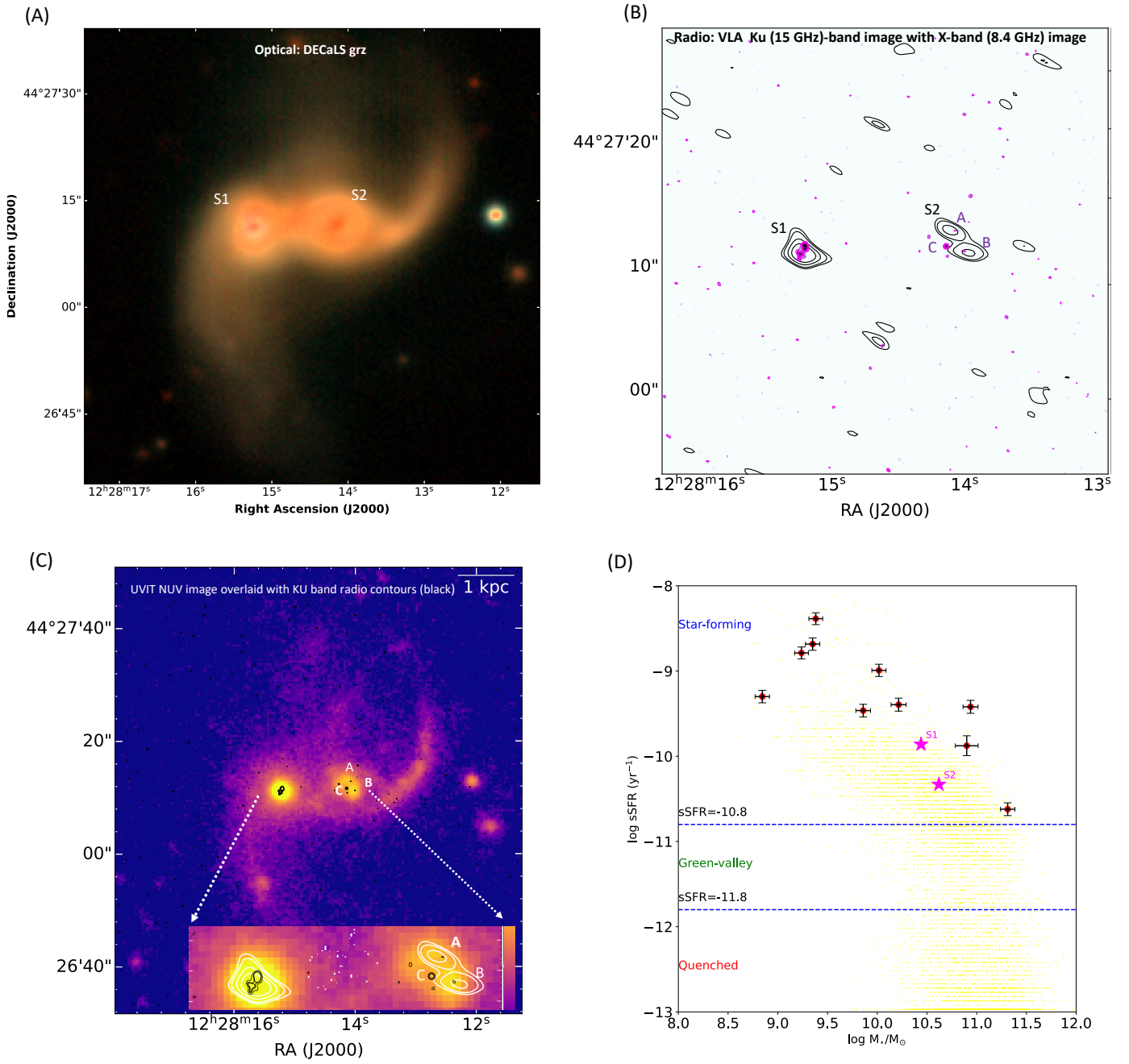


Figure 1. Multi-band images of MRK 212. Note that images are not at the same scale. **(A)** Optical color composite DECaLS image. The parent galaxies are defined as S1 and S2. The separation is ~ 5.6 kpc. **(B)** VLA X band contours overlaid with Ku-band (15 GHz) image and contours. The X-band contour levels are 20, 40, 60, and 80% of the peak flux density. Both sources S1 and S2 are detected. The extended structure is detected at 8.5 GHz (A, B), which is situated $1''$ (~ 500 pc) away from the optical center of S2. **(C)** The UVIT NUV image is overlaid with Ku-band 15 GHz radio contours (black). The inset shows a zoomed version of the radio structures. The NUV image revealed two clumps near the center of S2, which coincide with A and B in the radio 8.5 GHz image (white contours). The compact core (C) detected in the 15 GHz image associated with S2 coincides with the optical center. **(D)** The sSFR- M_* plot. Black points are all 10 dual-nuclei UVIT sample galaxies where MRK 212 (S1, S2) are shown with magenta star symbols. The data were adapted from [73,74] and images were reproduced.

An extended radio structure is detected in the 8.5 GHz VLA image (components A, B in Figure 1B, C). The spectral indices for components A and B are $\alpha = -0.53 \pm 0.10$

and -0.34 ± 0.10 , respectively [73]. The relatively flat spectral indices are consistent with the emission from SF regions where free-free emission could be mixed with synchrotron emission from supernovae. The UVIT NUV image shows UV bright knots (Figure 1C). These two clumps are situated $1''$ away from S2 and coincide with the radio-extended structure (A, B) at 8.5 GHz. The calculated SFR is higher compared to other selected regions on the disk or spiral arms. The 1.4 GHz uGMRT flux densities of A and B are 0.53 mJy and 0.37 mJy, respectively. As these clumps (A, B) are situated near the AGN nuclei S2 and on both sides, the star-formation in these clumps could have been triggered by the jet of S2 (if present) through AGN feedback. At the same time, these could be merger-induced star formation. A more sensitive high-resolution radio study could reveal a connection, if present, between the structures detected at 15 GHz and 8.4 GHz, and confirm or rule out the feedback scenario. The overall extinction corrected specific SFR (sSFR) and stellar mass (M_*) show that both S1 and S2 are actively star-forming systems in the galaxy main-sequence plot (purple stars: Figure 1D). This overlaps with the results found for the rest of the nine dual-nuclei galaxies of the sample (black points: Figure 1D) [74].

3. AGN Feedback in Radio-Quiet AGN

The majority of galaxies host radio-quiet AGN [93–97]. There are several questions related to radio-quiet sources that are still debatable, like the dominant process that produces radio emission, the mechanism through which they transfer energy, and their impact on the host galaxies [98,99].

Seyfert galaxies host radio-quiet AGN. Several Seyfert galaxies show kilo-parsec radio structures, which are sometimes distorted from the parsec scale structure [97]. A few Seyfert galaxies also show episodic AGN activity. Mrk6 exhibits a highly complex morphology: two pairs of self-similar bipolar bubble-like radio structures that are oriented nearly perpendicular to each other [100]. Another such example is NGC2992 [101]. However, most of these studies were performed with the GHz band observation, which can miss the total extent of radio emission as well as some emissions from the old epoch. Recently, a sample of Seyfert was observed with GMRT at 325 and 735 MHz to study the same (Rubinur et al. in preparation). One of the sample galaxies, NGC 2639, was studied with radio, UV, and CO data by [102].

3.1. Episodic AGN activity and feedback: NGC 2639

This is a Seyfert 2 type galaxy with a LINER (low-ionization nuclear emission-line region) like spectrum at a luminosity distance of 48.2 Mpc (redshift 0.01113) [103]. This galaxy hosts a SMBH of mass $M_{\text{BH}} = 1.48 \times 10^8 M_{\odot}$ [104] with an Eddington ratio 4×10^{-4} [102].

The uGMRT 735 MHz observation of NGC 2639 revealed a jet of size ~ 9 kpc (white contours in Figure 2A) in the NE–SW direction [102], while the 325 MHz image showed an unresolved structure in the same direction (Rubinur et al., in preparation). Rao et al. [102] proposed that the uGMRT detected jet (~ 9 kpc) was the fourth episode of AGN activity, as NGC 2639 is known to have hosted three episodes of AGN activity before [105]. These include a (i) 1.5 Kpc jet in the north–south direction (Black contours in Figure 2A); (ii) 360 pc jet in the east–west direction detected at 5 GHz VLA map (Figure 2B); and (iii) the 3pc jet detected with VLBA in the NE–SW direction (Figure 2C). These four jets do not show any connecting emissions and have clear hotspots or edges that distinguish them from each other.

The spectral age derived from BRATS (<https://www.askanastronomer.co.uk/brats/>) (Broadband Radio Astronomy Tools) found the age of the jet episodes with sizes of 9 kpc, 1.5 kpc, and 360 pc to be 34^{+4}_{-6} Myr, $11.8^{+1.7}_{-1.4}$ Myr, and $2.8^{+0.7}_{-0.5}$ Myr. These spectral ages proved the AGN jet duty cycle to be $\sim 60\%$. Sanders [106] proposed that Seyfert galaxies can have 100s of episodic AGN activity with a timescale 10^4 – 10^5 yr during their statistical lifetime of 3 – 7×10^8 yr. However, as mentioned earlier, episodic AGN activities are detected only in a few Seyfert galaxies, and the fourth episode in NGC 2639 is the highest number of detected epochs. This high-sensitivity uGMRT MHz observation shows that the detection

of episodic activity might be a matter of detecting low surface brightness emission from Seyfert/LINERs. While looking for the origin of these multiple jet episodes using the minor merger rate from the stellar mass and an assumed mass ratio, Rao et al. [102] found that the timescale favors three minor mergers that may have resulted in a new accretion disk and hence outflows.

The CARMA CO(1-0) (<https://mmwave.astro.illinois.edu/edgedata/>), GALEX FUV, and NUV images show a deficiency of molecular gas and UV emission in the central ~ 6 kpc of the galaxy, which is surrounded by a brighter ring (Figure 3). Using the molecular gas data from the CALIFA (Calar Alto Legacy Integral Field Area) (<https://califa.caha.es/>) survey, Ellison et al. [107] found that the central region of NGC 2639 has a lower gas fraction than the star-forming regions. This suggests that AGN has blown out the central molecular gas which leads to low star formation, as seen by GALEX data. Hence, evidence for a star-formation quenching phase is found in the central region of NGC 2639. Rao et al. [102] calculated the amount of work (pressure time volume PV) required to push the CO gas ring and the time-averaged power from 5 GHz flux densities. It turned out that only 0.5% of east–west jet power or a small fraction from the north–south jet would have been sufficient to push back the CO gas and create the hole.

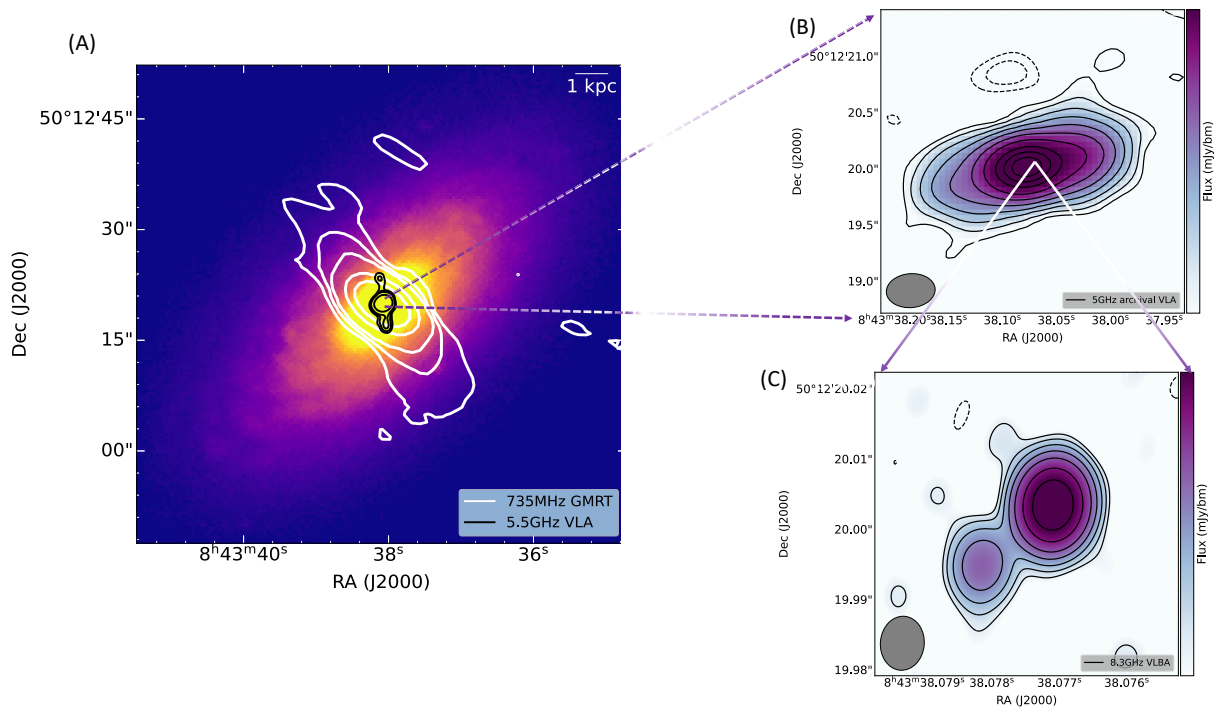


Figure 2. The four radio jet episodes of NGC2639. (A) The radio multi-band contours overlaid with the optical image. The color image is the SDSS r-band image. The white contours show the 735 MHz upgraded Giant Meterwave Telescope (uGMRT), which showed a jet of size ~ 9 kpc in the north–east–south–west direction. The beam of this image is $5.48 \text{ arcsec} \times 3.0 \text{ arcsec}$ at $\text{PA} = 54.6$ degrees. Contour levels: $(1, 2, 4, 32) \times 0.6 \text{ mJy beam}^{-1}$. The black contours are from the 5.5 GHz VLA total intensity image with the ~ 1.5 kpc jet in the north–south direction. The contour levels are $(2, 4, 8, 64) \times 0.03 \text{ mJy beam}^{-1}$ and the beam size is $1.02 \text{ arcsec} \times 0.89 \text{ arcsec}$ at $\text{PA} = -5.8$ degrees. (B) The 5 GHz VLA radio image with beam size $0.43 \text{ arcsec} \times 0.30 \text{ arcsec}$ at $\text{PA} = -85.4$ degrees. This image shows ~ 360 parsec lobe in the east–west direction. Contour levels: $(-2, -1, 1, 2, 4, 8, 16, 32, 64, 128) \times 0.164 \text{ mJy beam}^{-1}$. (C) The 8.3 GHz VLBA image with a beam size of $7.7 \text{ mas} \times 6.2 \text{ mas}$ at $\text{PA} = -4.9$ degrees. It shows ~ 3 parsec jet at $\text{PA} = 130$ degrees. Contour levels: $(-2, -1, 1, 2, 4, 8, 16, 32, 64) \times 0.239 \text{ mJy beam}^{-1}$. Data are adapted and figures are reproduced from Rao et al. [102], Sebastian et al. [105].

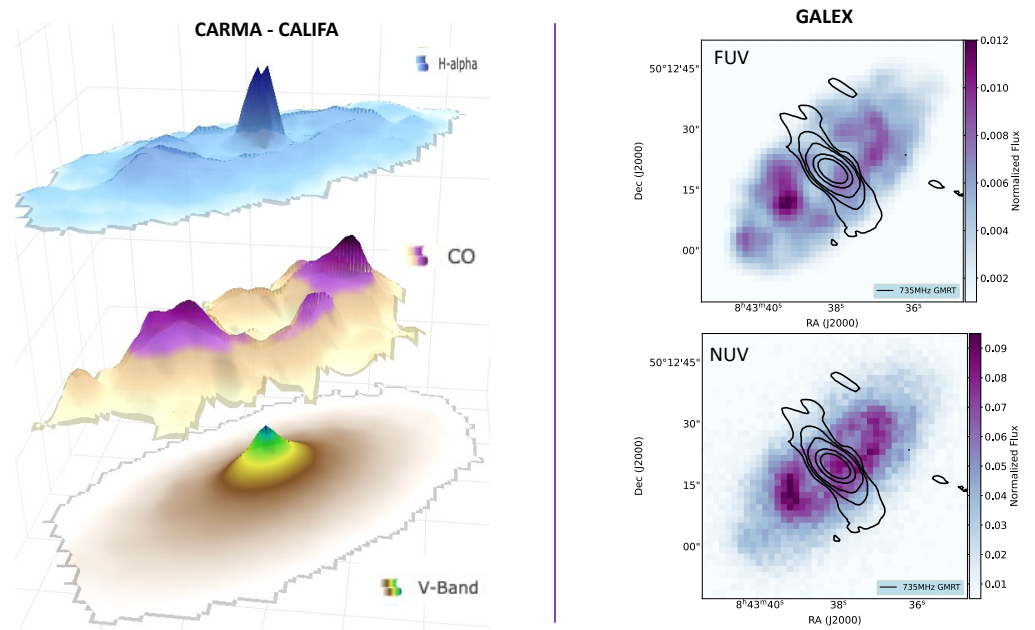


Figure 3. Multi-band images of NGC 2639 (**left**). This is a set of three-band images taken from the CARMA EDGE page for visualization: (**top**) the CALIFA $H\alpha$ image; (**middle**) the CO moment-0 map (**bottom**) V-band image; the CO(1-0) moment 0 map shows the deficiency at the central region of radius ~ 6 kpc. A hint of the same is seen in the $H\alpha$ image. (**right**) The GALEX FUV and NUV images overlaid with the uGMRT 735 MHz radio contours in black. The contour labels are the same as in Figure 2A. The central ~ 6 kpc shows a relative deficiency of FUV and NUV similar to the CO(1-0) map [102].

In NGC 7252 and the jellyfish galaxy JO201, AGN activities were found to suppress the star formation in the central region [108,109]. Both positive and negative feedback were observed in NGC 5728 [110]. The SFR surface density map from the GALEX NUV band showed a signature of suppressed SFR in the central region of NGC 3982 [111]. The Seyfert galaxy NGC 4051 shows the signature of multiple jet episodes [112,113], as well as a hole with a diameter of ~ 10 parsecs in its molecular gas distribution [114]. A recent MaNGA study [115] suggested that AGN feedback can significantly affect central star formation, but may be inefficient in driving galaxy-wide quenching in low-redshift galaxies. These studies showed that a detailed study of low-power AGN outflows, molecular gas, and star formation in radio-quiet galaxies with high resolution is important to understand feedback processes and their time scales.

3.2. Radio Loud Galaxies

Radio-loud brightest cluster galaxies (BCGs) have been found to show strong signatures of negative feedback from radio and X-ray data. Here, we look for signatures of jet-induced star formation in some of these objects from the literature. Very few such radio-loud objects show positive feedback: the examples in the nearby Universe are 3C 34 [116], 3C 285, and Minkowski's object (MO)[117]. 3C 34 is a radio galaxy with FR-II type AGN at redshift 0.69 [118]. It is situated in the center of a compact galaxy cluster, and the [OIII] line emission of the host galaxy is extended, which overlaps with the radio lobes [119]. Hubble Space Telescope (HST) images reveal a long blue optical emission in between the western lobe. Using fitted SED with a galaxy stellar population and spectral aging estimation of the radio jets, Best et al. [120] concluded that the supersonic shocks associated with the jet propagation induced the star formation on its path. 3C 285 is another double-lobed FR-II radio galaxy with a complex structure with filaments. The eastern lobe shows unresolved knots. An $H\alpha$ region known as 3C 285/09.6 [121] has been detected at a projected distance of 70 kpc on the eastern and shows jet-induced star formation. NGC 541,

a galaxy in the Abell 194 cluster, hosts double-lobed FR-I radio AGN. A star-forming region, known as Minkowski's Object (MO) is situated along the radio jet at a distance of 20 kpc [122] of NGC 541. The calculated SFR density, gas density, and depletion time support that star formation is triggered by the radio jet and hence supports positive feedback [117,123].

Centaurus A (Cen A: Figure 4) is a large radio source ($4^\circ \times 3^\circ$) hosted by the giant galaxy NGC 5128 [124,125]. This system has been studied through multi-band observations that revealed many interesting features, such as a warped disk and optical shells [126,127]. Recent simulations show that Cen A went through a merger approximately 2 Myr ago [128]. The radio structure shows radio lobes at different scales [129–132] (Figure 4B). The lobe at a distance of 15 kpc from the host galaxy is called the northern middle lobe (NML), which looks like an extension of the northern inner lobe (NIL) at a distance of about 8 kpc [133]. Different explanations exist for the origin of NML [134–136]. Cen A shows star formation along the jet, which is believed to be due to positive feedback [137,138] where the radio jet might interact with the gas around the NGC 5128 from the past merger activity [139]. However, it should be noted that the star-formation efficiency is quite low [140]. From the HI kinematics, Oosterloo and Morganti [141] found the signature of jet interaction with a large HI reservoir in the NE direction. UV bright filaments have been detected in the northern direction where young star clusters are also present. These filaments are known as inner and outer filaments, depending on the distance [136].

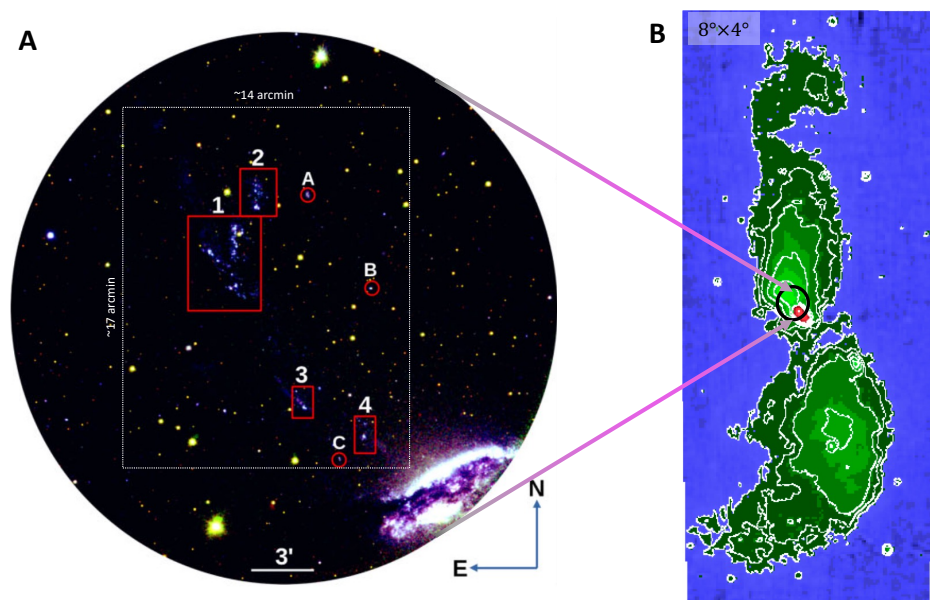


Figure 4. Image of Cen A: (left) color composite image with UVIT filters N245M in red, N219M in green, and F148W in blue colors. The circular image shows the 0.5-degree UVIT field of view. The scale is at the bottom. The Northern Star-forming Region (NSR) is shown in the dotted white box. The red boxes and the circular regions show a few interesting sources which were revealed by UVIT. Boxes 1 and 2 are part of the outer filament; Box 3 is part of the inner filament, and Box 4 shows new candidates for possible jet-induced star-forming sources. The circular regions A and C are UV sources, and a pair of stars are present in B. A detailed zoomed version of each thumbnail can be found in [142]. (right) The radio 6.3 cm total intensity image shows the full jet emission. These images are reproduced from [129,142].

Joseph et al. [142] studied the star-formation properties in the Northern Star-forming Region (NSR) of size 17×14 arcmin with the UVIT FUV and NUV multiple filters (F148W, N219M, and N245M) (white dotted box: Figure 4A). These UVIT observations revealed a complex structure of star-formation regions and some new candidates for star-forming regions. These images show that most of the UV bright objects are situated near the outer filament in a double structure, which is consistent with a two-segment structure: a V-shaped

segment and an elongated segment. Fewer UV sources are observed near the inner filament compared to the outer filament, and they show an elongated structure. There is also UV emission present between the inner filament and NGC 5128. After excluding the Galactic sources and background galaxies, 83 star-forming regions were detected, of which 61 are situated in outer regions and 16 are in inner regions. They compared these star-forming structures with radio images and used the *starburst99* [143] model and FUV-NUV color to estimate the age of the star-forming sources. The main findings were (i) the star-forming structure is along the jet vector, (ii) two distinct populations of stars are present in inner and outer regions, which may have two different origins, and (iii) a catalog including new UV sources likely connected to Cen A was provided [142].

4C 41.17 is one of the best studied radio galaxies at $z = 3.79$ [144] and shows jet-induced star-formation at high redshift. Recently, regarding the gas mass density and SFR surface density of 4C 41.17, Nesvadba et al. [145] found that the jets are not currently forming stars and they argued that radio jets help in star formation, but without enhancing it, especially after the jet has broken out of the interstellar medium.

Recently, LOFAR 144 MHz images revealed a large-scale radio plume in the central galaxy GIN 049 in galaxy cluster Abell A160 that passes through the spiral galaxy J036 [146]. Further investigation of this system with uGMRT and MUSE data showed that the radio plume of GI 049 interacted with JO36 in the past 200–500 Myr, which resulted in a burst of star formation with $\text{SFR } 14 \text{ M}_{\odot} \text{ yr}^{-1}$. This is another example of positive feedback [146].

4. Summary and Future Scope with UV Telescopes

In this article, we discussed the signatures of AGN feedback, mainly focusing on the alignment between observed radio and UV emission. However, it should be noted that it was not possible to include all AGN feedback-related discoveries from all the existing UV telescopes. The presented works are mainly from UVIT [73,111] and GALEX [102]. A few studies that used HST UV data are also mentioned [45,50]. The high-resolution UV data have detected star-forming clumps near the nuclei of MRK 212 showing a signature of possible positive AGN feedback. The UV deficiency in the center of NGC 2639 suggests AGN negative feedback. These studies show that detailed high-resolution multi-frequency observations of a large sample of galaxy mergers and radio-quiet galaxies are important for understanding the feedback effect throughout the lifetime of the galaxies. The detection of a fourth episodic jet of NGC 2639 from uGMRT also shows the importance of high-resolution, high-sensitive low-frequency radio observations. The detailed study of Cen A star-forming regions revealed two distinct stellar populations and new star-forming regions that might be triggered by the jet [111].

Next, we briefly discuss upcoming UV missions that are expected to provide better images and spectra in this field. The HST has been providing high-resolution images (in both UV and optical) and spectra since the 1990s. However, the field of view is very small (0.002 deg^2) and the HST is approaching the end of its lifetime. The GALEX mission, which worked between 2003 and 2013, had a resolution resolution of $5''$ and a FOV of 1.4 deg^2 . The UVIT has been providing images with $\sim 1.5''$ resolution since the launch of Astrosat in 2015. Initially, it was planned to have a 5-year lifespan. However, some of the filters are still working and providing good results. A future UV mission, INdian Spectroscopic and Imaging Space Telescope (INSIST; PI: Annapurni Subramaniam: [147]) has been approved by the Indian Space Research Organisation (ISRO) (<https://www.isro.gov.in/>) in 2019. This is an observatory-class mission with an expected resolution of $\sim 0.2''$, FOV of $\sim 5' - 15'$ and a detection limit of $\sim 26 \text{ mag}$ in UV for an exposure time of 1 kilosec. More details about the instruments of the mission can be found in [147]. Ultraviolet Explorer (UVEX) is NASA's upcoming mission, targeted in 2030. This is a medium-class explorer mission (<https://www.ipac.caltech.edu/project/uvex>). UVEX will also have imaging and spectroscopy in both NUV and FUV bands. This is a dedicated mission for an all-sky survey in UV, with an expected PSF size of $2.5''$ and a FOV of 12 deg^2 . This is expected to

make 50/100-times deeper images than GALEX, as well as to provide spectroscopy with a resolution of ~ 1000 .

Both INSIST [147] and UVEX [148] are motivated by strong scientific goals, which include understanding galaxy formation and evolution, the nuclei of galaxies, stellar populations, transients, large sky survey, etc. AGN feedback is an important part of galaxy evolution and a slowly emerging picture is that both positive and negative feedback may be present in galaxies coupled with galaxy mergers or secular and environmental processes. In addition, AGN feedback may work differently in different objects (like radio-loud and radio-quiet) and in different time scales. Here, the future instruments INSIST and UVEX in the UV band will play a crucial role, along with JWST (<https://webb.nasa.gov/>), LSST (<https://www.lsst.org/>), and EUCLID (<https://www.euclid-ec.org/>) in other bands.

Funding: This research received no external funding

Institutional Review Board Statement: Not applicable

Informed Consent Statement: Not applicable.

Data Availability Statement: The data underlying this article will be shared on reasonable request to the corresponding author.

Acknowledgments: We would like to thank the “AGN on the beach” Tropea, Italy, organizers. We thank the anonymous reviewers for their suggestions that have significantly improved this paper. We want to acknowledge the help received from the Institute of Theoretical Astrophysics (ITA) at the University of Oslo. RK wants to thank N. Junkes for sharing the total intensity radio maps from Parkes radio telescope observations of Cen A. This publication uses data from the AstroSat mission of the Indian Space Research Organisation (ISRO), archived at the Indian Space Science Data Centre (ISSDC), which is a result of collaboration between IIA, Bengaluru, IUCAA, Pune, TIFR, Mumbai, several centers of ISRO, and CSA. GMRT is run by the National Centre for Radio Astrophysics of the Tata Institute of Fundamental Research. RK wants to thank Prasanta Kumar Nayak, Prajwel Joseph, Mousumi Das, Avijeet Prasad, and Akhil Lasrado for productive discussions.

Conflicts of Interest: The author declares no conflict of interest.

References

1. Madau, P.; Dickinson, M. Cosmic Star-Formation History. *Annu. Rev. Astron. Astrophys.* **2014**, *52*, 415–486. <https://doi.org/10.1146/annurev-astro-081811-125615>.
2. Ferrarese, L.; Merritt, D. A Fundamental Relation between Supermassive Black Holes and Their Host Galaxies. *Astrophys. J.* **2000**, *539*, L9–L12. <https://doi.org/10.1086/312838>.
3. Gültekin, K.; Richstone, D.O.; Gebhardt, K.; Lauer, T.R.; Tremaine, S.; Aller, M.C.; Bender, R.; Dressler, A.; Faber, S.M.; Filippenko, A.V.; et al. The $M-\sigma$ and $M-L$ Relations in Galactic Bulges, and Determinations of Their Intrinsic Scatter. *Astrophys. J.* **2009**, *698*, 198–221. <https://doi.org/10.1088/0004-637X/698/1/198>.
4. Kormendy, J.; Ho, L.C. Coevolution (Or Not) of Supermassive Black Holes and Host Galaxies. *Annu. Rev. Astron. Astrophys.* **2013**, *51*, 511–653. <https://doi.org/10.1146/annurev-astro-082708-101811>.
5. Fabian, A.C. Observational Evidence of Active Galactic Nuclei Feedback. *Annu. Rev. Astron. Astrophys.* **2012**, *50*, 455–489. <https://doi.org/10.1146/annurev-astro-081811-125521>.
6. Cattaneo, A.; Faber, S.M.; Binney, J.; Dekel, A.; Kormendy, J.; Mushotzky, R.; Babul, A.; Best, P.N.; Brüggen, M.; Fabian, A.C.; et al. The role of black holes in galaxy formation and evolution. *Nature* **2009**, *460*, 213–219. <https://doi.org/10.1038/nature08135>.
7. Alexander, D.M.; Hickox, R.C. What drives the growth of black holes? *New Astron. Rev.* **2012**, *56*, 93–121. <https://doi.org/10.1016/j.newar.2011.11.003>.
8. King, A.; Pounds, K. Powerful Outflows and Feedback from Active Galactic Nuclei. *Annu. Rev. Astron. Astrophys.* **2015**, *53*, 115–154. <https://doi.org/10.1146/annurev-astro-082214-122316>.
9. Morganti, R. The many routes to AGN feedback. *Front. Astron. Space Sci.* **2017**, *4*, 42. <https://doi.org/10.3389/fspas.2017.00042>.
10. Di Matteo, T.; Springel, V.; Hernquist, L. Energy input from quasars regulates the growth and activity of black holes and their host galaxies. *Nature* **2005**, *433*, 604–607. <https://doi.org/10.1038/nature03335>.
11. Baldry, I.K.; Balogh, M.L.; Bower, R.G.; Glazebrook, K.; Nichol, R.C.; Bamford, S.P.; Budavari, T. Galaxy bimodality versus stellar mass and environment. *Mon. Not. R. Astron. Soc.* **2006**, *373*, 469–483. <https://doi.org/10.1111/j.1365-2966.2006.11081.x>.
12. Dubois, Y.; Devriendt, J.; Slyz, A.; Teyssier, R. Self-regulated growth of supermassive black holes by a dual jet-heating active galactic nucleus feedback mechanism: Methods, tests and implications for cosmological simulations. *Mon. Not. R. Astron. Soc.* **2012**, *420*, 2662–2683. <https://doi.org/10.1111/j.1365-2966.2011.20236.x>.

13. Silk, J.; Mamon, G.A. The current status of galaxy formation. *Res. Astron. Astrophys.* **2012**, *12*, 917–946. <https://doi.org/10.1088/1674-4527/12/8/004>.
14. Choi, E.; Somerville, R.S.; Ostriker, J.P.; Naab, T.; Hirschmann, M. The Role of Black Hole Feedback on Size and Structural Evolution in Massive Galaxies. *Astrophys. J.* **2018**, *866*, 91. <https://doi.org/10.3847/1538-4357/aae076>.
15. Davé, R.; Anglés-Alcázar, D.; Narayanan, D.; Li, Q.; Rafieferantsoa, M.H.; Appleby, S. SIMBA: Cosmological simulations with black hole growth and feedback. *Mon. Not. R. Astron. Soc.* **2019**, *486*, 2827–2849. <https://doi.org/10.1093/mnras/stz937>.
16. McNamara, B.R.; Nulsen, P.E.J. Heating Hot Atmospheres with Active Galactic Nuclei. *Annu. Rev. Astron. Astrophys.* **2007**, *45*, 117–175. <https://doi.org/10.1146/annurev.astro.45.051806.110625>.
17. McNamara, B.R.; Nulsen, P.E.J. Mechanical feedback from active galactic nuclei in galaxies, groups and clusters. *New J. Phys.* **2012**, *14*, 055023. <https://doi.org/10.1088/1367-2630/14/5/055023>.
18. Nulsen, P.E.J.; Jones, C.; Forman, W.R.; David, L.P.; McNamara, B.R.; Rafferty, D.A.; Birzan, L.; Wise, M.W. AGN Heating Through Cavities and Shocks. In *Heating versus Cooling in Galaxies and Clusters of Galaxies*; Böhringer, H., Pratt, G.W., Finoguenov, A., Schuecker, P., Eds.; 2007, Eso Astrophysics Symposia; Springer-Verlag Berlin Heidelberg; p. 210. https://doi.org/10.1007/978-3-540-73484-0_37.
19. Cavagnolo, K.W.; McNamara, B.R.; Nulsen, P.E.J.; Carilli, C.L.; Jones, C.; Birzan, L. A Relationship Between AGN Jet Power and Radio Power. *Astrophys. J.* **2010**, *720*, 1066–1072. <https://doi.org/10.1088/0004-637X/720/2/1066>.
20. Faucher-Giguère, C.A.; Quataert, E. The physics of galactic winds driven by active galactic nuclei. *Mon. Not. R. Astron. Soc.* **2012**, *425*, 605–622. <https://doi.org/10.1111/j.1365-2966.2012.21512.x>.
21. Costa, T.; Sijacki, D.; Trenti, M.; Haehnelt, M.G. The environment of bright QSOs at $z \sim 6$: star-forming galaxies and X-ray emission. *Mon. Not. R. Astron. Soc.* **2014**, *439*, 2146–2174. <https://doi.org/10.1093/mnras/stu101>.
22. Mahony, E.K.; Morganti, R.; Emonts, B.H.C.; Oosterloo, T.A.; Tadhunter, C. The location and impact of jet-driven outflows of cold gas: the case of 3C 293. *Mon. Not. R. Astron. Soc.* **2013**, *435*, L58–L62. <https://doi.org/10.1093/mnras/slt094>.
23. Hardcastle, M.J.; Croston, J.H. Radio galaxies and feedback from AGN jets. *New Astron. Rev.* **2020**, *88*, 101539. <https://doi.org/10.1016/j.newar.2020.101539>.
24. Ishibashi, W.; Fabian, A.C. Active galactic nucleus feedback and triggering of star formation in galaxies. *Mon. Not. R. Astron. Soc.* **2012**, *427*, 2998–3005. <https://doi.org/10.1111/j.1365-2966.2012.22074.x>.
25. Zubovas, K.; Nayakshin, S.; Sazonov, S.; Sunyaev, R. Outflows of stars due to quasar feedback. *Mon. Not. R. Astron. Soc.* **2013**, *431*, 793–798. <https://doi.org/10.1093/mnras/stt214>.
26. Rupke, D.S.; Veilleux, S.; Sanders, D.B. Outflows in Active Galactic Nucleus/Starburst-Composite Ultraluminous Infrared Galaxies I. *Astrophys. J.* **2005**, *632*, 751–780. <https://doi.org/10.1086/444451>.
27. Rupke, D.S.N.; Veilleux, S. The Multiphase Structure and Power Sources of Galactic Winds in Major Mergers. *Astrophys. J.* **2013**, *768*, 75. <https://doi.org/10.1088/0004-637X/768/1/75>.
28. Liu, G.; Zakamska, N.L.; Greene, J.E.; Nesvadba, N.P.H.; Liu, X. Observations of feedback from radio-quiet quasars—II. Kinematics of ionized gas nebulae. *Mon. Not. R. Astron. Soc.* **2013**, *436*, 2576–2597. <https://doi.org/10.1093/mnras/stt1755>.
29. Cicone, C.; Maiolino, R.; Sturm, E.; Graciá-Carpio, J.; Feruglio, C.; Neri, R.; Aalto, S.; Davies, R.; Fiore, F.; Fischer, J.; et al. Massive molecular outflows and evidence for AGN feedback from CO observations. *Astron. Astrophys.* **2014**, *562*, A21. <https://doi.org/10.1051/0004-6361/201322464>.
30. Harrison, C.M.; Costa, T.; Tadhunter, C.N.; Flütsch, A.; Kakkad, D.; Perna, M.; Vietri, G. AGN outflows and feedback twenty years on. *Nat. Astron.* **2018**, *2*, 198–205. <https://doi.org/10.1038/s41550-018-0403-6>.
31. Roy, N.; Bundy, K.; Rubin, K.H.R.; Rowlands, K.; Westfall, K.; Riffel, R.; Bizyaev, D.; Stark, D.V.; Riffel, R.A.; Lacerna, I.; et al. Signatures of Inflowing Gas in Red Geyser Galaxies Hosting Radio Active Galactic Nuclei. *Astrophys. J.* **2021**, *919*, 145. <https://doi.org/10.3847/1538-4357/ac0f74>.
32. Venturi, G.; Cresci, G.; Marconi, A.; Mingozzi, M.; Nardini, E.; Carniani, S.; Mannucci, F.; Marasco, A.; Maiolino, R.; Perna, M.; et al. MAGNUM survey: Compact jets causing large turmoil in galaxies. Enhanced line widths perpendicular to radio jets as tracers of jet-ISM interaction. *Astron. Astrophys.* **2021**, *648*, A17. <https://doi.org/10.1051/0004-6361/202039869>.
33. Ramos Almeida, C.; Bischetti, M.; García-Burillo, S.; Alonso-Herrero, A.; Audibert, A.; Cicone, C.; Feruglio, C.; Tadhunter, C.N.; Pierce, J.C.S.; Pereira-Santaella, M.; et al. The diverse cold molecular gas contents, morphologies, and kinematics of type-2 quasars as seen by ALMA. *Astron. Astrophys.* **2022**, *658*, A155. <https://doi.org/10.1051/0004-6361/202141906>.
34. Fischer, J.; Sturm, E.; González-Alfonso, E.; Graciá-Carpio, J.; Hailey-Dunsheath, S.; Poglitsch, A.; Contursi, A.; Lutz, D.; Genzel, R.; Sternberg, A.; et al. Herschel-PACS spectroscopic diagnostics of local ULIRGs: Conditions and kinematics in Markarian 231. *Astron. Astrophys.* **2010**, *518*, L41. <https://doi.org/10.1051/0004-6361/201014676>.
35. Oosterloo, T.A.; Morganti, R.; Tzioumis, A.; Reynolds, J.; King, E.; McCulloch, P.; Tsvetanov, Z. A Strong Jet-Cloud Interaction in the Seyfert Galaxy IC 5063: VLBI Observations. *Astron. J.* **2000**, *119*, 2085–2091. <https://doi.org/10.1086/301358>.
36. Cicone, C.; Feruglio, C.; Maiolino, R.; Fiore, F.; Piconcelli, E.; Menci, N.; Aussel, H.; Sturm, E. The physics and the structure of the quasar-driven outflow in Mrk 231. *Astron. Astrophys.* **2012**, *543*, A99. <https://doi.org/10.1051/0004-6361/201218793>.
37. Feruglio, C.; Fiore, F.; Carniani, S.; Piconcelli, E.; Zappacosta, L.; Bongiorno, A.; Cicone, C.; Maiolino, R.; Marconi, A.; Menci, N.; et al. The multi-phase winds of Markarian 231: from the hot, nuclear, ultra-fast wind to the galaxy-scale, molecular outflow. *Astron. Astrophys.* **2015**, *583*, A99. <https://doi.org/10.1051/0004-6361/201526020>.

38. Morganti, R.; Veilleux, S.; Oosterloo, T.; Teng, S.H.; Rupke, D. Another piece of the puzzle: The fast H I outflow in Mrk 231. *Astron. Astrophys.* **2016**, *593*, A30. <https://doi.org/10.1051/0004-6361/201628978>.
39. Dasyra, K.M.; Combes, F.; Oosterloo, T.; Oonk, J.B.R.; Morganti, R.; Salomé, P.; Vlahakis, N. ALMA reveals optically thin, highly excited CO gas in the jet-driven winds of the galaxy IC 5063. *Astron. Astrophys.* **2016**, *595*, L7. <https://doi.org/10.1051/0004-6361/201629689>.
40. Tadhunter, C.; Morganti, R.; Rose, M.; Oonk, J.B.R.; Oosterloo, T. Jet acceleration of the fast molecular outflows in the Seyfert galaxy IC 5063. *Nature* **2014**, *511*, 440–443. <https://doi.org/10.1038/nature13520>.
41. Morganti, R.; Oosterloo, T.; Oonk, J.B.R.; Frieswijk, W.; Tadhunter, C. The fast molecular outflow in the Seyfert galaxy IC 5063 as seen by ALMA. *Astron. Astrophys.* **2015**, *580*, A1. <https://doi.org/10.1051/0004-6361/201525860>.
42. Maiolino, R.; Russell, H.R.; Fabian, A.C.; Carniani, S.; Gallagher, R.; Cazzoli, S.; Arribas, S.; Belfiore, F.; Bellocchi, E.; Colina, L.; et al. Star formation inside a galactic outflow. *Nature* **2017**, *544*, 202–206. <https://doi.org/10.1038/nature21677>.
43. Gallagher, R.; Maiolino, R.; Belfiore, F.; Drory, N.; Riffel, R.; Riffel, R.A. Widespread star formation inside galactic outflows. *Mon. Not. R. Astron. Soc.* **2019**, *485*, 3409–3429. <https://doi.org/10.1093/mnras/stz564>.
44. Mukherjee, D.; Bicknell, G.V.; Wagner, A.Y.; Sutherland, R.S.; Silk, J. Relativistic jet feedback—III. Feedback on gas discs. *Mon. Not. R. Astron. Soc.* **2018**, *479*, 5544–5566. <https://doi.org/10.1093/mnras/sty1776>.
45. Tamhane, P.D.; McNamara, B.R.; Russell, H.R.; Combes, F.; Qiu, Y.; Edge, A.C.; Maiolino, R.; Fabian, A.C.; Nulsen, P.E.J.; Johnstone, R.; et al. Radio jet-ISM interaction and positive radio-mechanical feedback in Abell 1795. *Mon. Not. R. Astron. Soc.* **2023**, *519*, 3338–3356. <https://doi.org/10.1093/mnras/stac3803>.
46. Zirm, A.W.; Overzier, R.A.; Miley, G.K.; Blakeslee, J.P.; Clampin, M.; De Breuck, C.; Demarco, R.; Ford, H.C.; Hartig, G.F.; Homeier, N.; et al. Feedback and Brightest Cluster Galaxy Formation: ACS Observations of the Radio Galaxy TN J1338-1942 at $z = 4.1$. *Astrophys. J.* **2005**, *630*, 68–81. <https://doi.org/10.1086/431921>.
47. Drouart, G.; Rocca-Volmerange, B.; De Breuck, C.; Fioc, M.; Lehnert, M.; Seymour, N.; Stern, D.; Vernet, J. Disentangling star formation and AGN activity in powerful infrared luminous radio galaxies at $1 < z < 4$. *Astron. Astrophys.* **2016**, *593*, A109. <https://doi.org/10.1051/0004-6361/201526880>.
48. Kennicutt, R.C. Star Formation in Galaxies Along the Hubble Sequence. *Annu. Rev. Astron. Astrophys.* **1998**, *36*, 189–232. <https://doi.org/10.1146/annurev.astro.36.1.189>.
49. Calzetti, D. Star Formation Rate Indicators. In *Secular Evolution of Galaxies*; Falcón-Barroso, J., Knapen, J.H., Eds.; 2013; Proceedings of the XXIII Canary Islands Winter School of Astrophysics: ‘Secular Evolution of Galaxies’; Cambridge University Press; p. 419.
50. Duggal, C.; O’Dea, C.P.; Baum, S.A.; Labiano, A.; Tadhunter, C.; Worrall, D.M.; Morganti, R.; Tremblay, G.R.; Dicken, D. Optical- & UV-Continuum Morphologies of Compact Radio Source Hosts. *arXiv* **2023**, arXiv:2309.00110. <https://doi.org/10.48550/arXiv.2309.00110>.
51. Kumar, A.; Ghosh, S.K.; Hutchings, J.; Kamath, P.U.; Kathiravan, S.; Mahesh, P.K.; Murthy, J.; Nagbhushana, S.; Pati, A.K.; Rao, M.N.; et al. Ultra Violet Imaging Telescope (UVIT) on ASTROSAT. In *Society of Photo-Optical Instrumentation Engineers (SPIE) Conference Series*; 2012; , Space Telescopes and Instrumentation 2012: Ultraviolet to Gamma Ray, Bellingham, Volume 8443, p. 84431N. <https://doi.org/10.1117/12.924507>.
52. Martin, D.C.; Fanson, J.; Schiminovich, D.; Morrissey, P.; Friedman, P.G.; Barlow, T.A.; Conrow, T.; Grange, R.; Jelinsky, P.N.; Milliand, B.; et al. The Galaxy Evolution Explorer: A Space Ultraviolet Survey Mission. *Astrophys. J.* **2005**, *619*, L1–L6. <https://doi.org/10.1086/426387>.
53. Daddi, E.; Dickinson, M.; Morrison, G.; Chary, R.; Cimatti, A.; Elbaz, D.; Frayer, D.; Renzini, A.; Pope, A.; Alexander, D.M.; et al. Multiwavelength Study of Massive Galaxies at $z \sim 2$. I. Star Formation and Galaxy Growth. *Astrophys. J.* **2007**, *670*, 156–172. <https://doi.org/10.1086/521818>.
54. Salim, S.; Rich, R.M.; Charlot, S.; Brinchmann, J.; Johnson, B.D.; Schiminovich, D.; Seibert, M.; Mallery, R.; Heckman, T.M.; Forster, K.; et al. UV Star Formation Rates in the Local Universe. *Astrophys. J. Suppl. Ser.* **2007**, *173*, 267–292. <https://doi.org/10.1086/519218>.
55. Tomczak, A.R.; Quadri, R.F.; Tran, K.V.H.; Labbé, I.; Straatman, C.M.S.; Papovich, C.; Glazebrook, K.; Allen, R.; Brammer, G.B.; Cowley, M.; et al. The SFR-M* Relation and Empirical Star-Formation Histories from ZFOURGE* at $0.5 < z < 4$. *Astrophys. J.* **2016**, *817*, 118. <https://doi.org/10.3847/0004-637X/817/2/118>.
56. Elbaz, D.; Leiton, R.; Nagar, N.; Okumura, K.; Franco, M.; Schreiber, C.; Pannella, M.; Wang, T.; Dickinson, M.; Díaz-Santos, T.; et al. Starbursts in and out of the star-formation main sequence. *Astron. Astrophys.* **2018**, *616*, A110. <https://doi.org/10.1051/0004-6361/201732370>.
57. Schawinski, K.; Khochfar, S.; Kaviraj, S.; Yi, S.K.; Boselli, A.; Barlow, T.; Conrow, T.; Forster, K.; Friedman, P.G.; Martin, D.C.; et al. Suppression of star formation in early-type galaxies by feedback from supermassive black holes. *Nature* **2006**, *442*, 888–891. <https://doi.org/10.1038/nature04934>.
58. Hickox, R.C.; Jones, C.; Forman, W.R.; Murray, S.S.; Kochanek, C.S.; Eisenstein, D.; Jannuzi, B.T.; Dey, A.; Brown, M.J.I.; Stern, D.; et al. Host Galaxies, Clustering, Eddington Ratios, and Evolution of Radio, X-Ray, and Infrared-Selected AGNs. *Astrophys. J.* **2009**, *696*, 891–919. <https://doi.org/10.1088/0004-637X/696/1/891>.
59. Kaviraj, S.; Laigle, C.; Kimm, T.; Devriendt, J.E.G.; Dubois, Y.; Pichon, C.; Slyz, A.; Chisari, E.; Peirani, S. The Horizon-AGN simulation: evolution of galaxy properties over cosmic time. *Mon. Not. R. Astron. Soc.* **2017**, *467*, 4739–4752. <https://doi.org/10.1093/mnras/stx126>.

60. Volonteri, M.; Haardt, F.; Madau, P. The Assembly and Merging History of Supermassive Black Holes in Hierarchical Models of Galaxy Formation. *Astrophys. J.* **2003**, *582*, 559–573. <https://doi.org/10.1086/344675>.
61. Springel, V. The cosmological simulation code GADGET-2. *Mon. Not. R. Astron. Soc.* **2005**, *364*, 1105–1134. <https://doi.org/10.1111/j.1365-2966.2005.09655.x>.
62. Faisst, A.L.; Carollo, C.M.; Capak, P.L.; Tacchella, S.; Renzini, A.; Ilbert, O.; McCracken, H.J.; Scoville, N.Z. Constraints on Quenching of $Z \lesssim 2$ Massive Galaxies from the Evolution of the Average Sizes of Star-forming and Quenched Populations in COSMOS. *Astrophys. J.* **2017**, *839*, 71. <https://doi.org/10.3847/1538-4357/aa697a>.
63. Gunn, J.E.; Gott, J. Richard, I. On the Infall of Matter Into Clusters of Galaxies and Some Effects on Their Evolution. *Astrophys. J.* **1972**, *176*, 1. <https://doi.org/10.1086/151605>.
64. Barnes, J.E.; Hernquist, L. Dynamics of interacting galaxies. *Annu. Rev. Astron. Astrophys.* **1992**, *30*, 705–742. <https://doi.org/10.1146/annurev.aa.30.090192.003421>.
65. Bournaud, F. Star Formation and Structure Formation in Galaxy Interactions and Mergers. In Proceedings of the Galaxy Wars: Stellar Populations and Star Formation in Interacting Galaxies ASP Conference Series; proceedings of a conference held 19–22 July 2009 at East Tennessee State University, Johnson City, Tennessee, USA.; Smith, B., Higdon, J., Higdon, S., Bastian, N., Eds.; *Astronomical Society of the Pacific Conference Series*; 2010; Volume 423, p. 177. <http://arxiv.org/abs/0909.1812>.
66. Hopkins, P.F.; Hernquist, L.; Cox, T.J.; Di Matteo, T.; Robertson, B.; Springel, V. A Unified, Merger-driven Model of the Origin of Starbursts, Quasars, the Cosmic X-Ray Background, Supermassive Black Holes, and Galaxy Spheroids. *Astrophys. J. Suppl. Ser.* **2006**, *163*, 1–49. <https://doi.org/10.1086/499298>.
67. Ellison, S.L.; Patton, D.R.; Mendel, J.T.; Scudder, J.M. Galaxy pairs in the Sloan Digital Sky Survey—IV. Interactions trigger active galactic nuclei. *Mon. Not. R. Astron. Soc.* **2011**, *418*, 2043–2053. <https://doi.org/10.1111/j.1365-2966.2011.19624.x>.
68. Satyapal, S.; Ellison, S.L.; McAlpine, W.; Hickox, R.C.; Patton, D.R.; Mendel, J.T. Galaxy pairs in the Sloan Digital Sky Survey—IX. Merger-induced AGN activity as traced by the Wide-field Infrared Survey Explorer. *Mon. Not. R. Astron. Soc.* **2014**, *441*, 1297–1304. <https://doi.org/10.1093/mnras/stu650>.
69. Kaviraj, S.; Martin, G.; Silk, J. AGN in dwarf galaxies: Frequency, triggering processes and the plausibility of AGN feedback. *Mon. Not. R. Astron. Soc.* **2019**, *489*, L12–L16. <https://doi.org/10.1093/mnrasl/slz102>.
70. Cazzoli, S. Negative and positive outflow-feedback in nearby (U)LIRGs. *Front. Astron. Space Sci.* **2017**, *4*, 62. <https://doi.org/10.3389/fspas.2017.00062>.
71. Springel, V.; Di Matteo, T.; Hernquist, L. Black Holes in Galaxy Mergers: The Formation of Red Elliptical Galaxies. *Astrophys. J.* **2005**, *620*, L79–L82. <https://doi.org/10.1086/428772>.
72. Sparre, M.; Springel, V. The unorthodox evolution of major merger remnants into star-forming spiral galaxies. *Mon. Not. R. Astron. Soc.* **2017**, *470*, 3946–3958. <https://doi.org/10.1093/mnras/stx1516>.
73. Rubinur, K.; Kharb, P.; Das, M.; Rahna, P.T.; Honey, M.; Paswan, A.; Vaddi, S.; Murthy, J. A multiwavelength study of the dual nuclei in Mrk 212. *Mon. Not. R. Astron. Soc.* **2021**, *500*, 3908–3919. <https://doi.org/10.1093/mnras/staa3375>.
74. Rubinur, K.; Das, M.; Kharb, P.; Yadav, J.; Mondal, C.; Rahna, P.T. Study of star formation in dual nuclei galaxies using UVIT observations. *Mon. Not. R. Astron. Soc.* **2024**, *528*, 4432–4450. <https://doi.org/10.1093/mnras/stae318>.
75. Baldwin, J.A.; Phillips, M.M.; Terlevich, R. Classification parameters for the emission-line spectra of extragalactic objects. *Publ. Astron. Soc. Pac.* **1981**, *93*, 5–19. <https://doi.org/10.1086/130766>.
76. Satyapal, S.; Secrest, N.J.; Ricci, C.; Ellison, S.L.; Rothberg, B.; Blecha, L.; Constantin, A.; Gliozzi, M.; McNulty, P.; Ferguson, J. Buried AGNs in Advanced Mergers: Mid-infrared Color Selection as a Dual AGN Candidate Finder. *Astrophys. J.* **2017**, *848*, 126. <https://doi.org/10.3847/1538-4357/aa88ca>.
77. Agostino, C.J.; Salim, S. Crossing the Line: Active Galactic Nuclei in the Star-forming Region of the BPT Diagram. *Astrophys. J.* **2019**, *876*, 12. <https://doi.org/10.3847/1538-4357/ab1094>.
78. Begelman, M.C.; Blandford, R.D.; Rees, M.J. Massive black hole binaries in active galactic nuclei. *Nature* **1980**, *287*, 307–309. <https://doi.org/10.1038/287307a0>.
79. Komossa, S.; Burwitz, V.; Hasinger, G.; Predehl, P.; Kaastra, J.S.; Ikebe, Y. Discovery of a Binary Active Galactic Nucleus in the Ultraluminous Infrared Galaxy NGC 6240 Using Chandra. *Astrophys. J.* **2003**, *582*, L15–L19. <https://doi.org/10.1086/346145>.
80. Comerford, J.M.; Gerke, B.F.; Stern, D.; Cooper, M.C.; Weiner, B.J.; Newman, J.A.; Madsen, K.; Barrows, R.S. Kiloparsec-scale Spatial Offsets in Double-peaked Narrow-line Active Galactic Nuclei. I. Markers for Selection of Compelling Dual Active Galactic Nucleus Candidates. *Astrophys. J.* **2012**, *753*, 42. <https://doi.org/10.1088/0004-637X/753/1/42>.
81. Müller-Sánchez, F.; Comerford, J.M.; Nevin, R.; Barrows, R.S.; Cooper, M.C.; Greene, J.E. The Origin of Double-peaked Narrow Lines in Active Galactic Nuclei. I. Very Large Array Detections of Dual AGNs and AGN Outflows. *Astrophys. J.* **2015**, *813*, 103. <https://doi.org/10.1088/0004-637X/813/2/103>.
82. Rubinur, K.; Das, M.; Kharb, P. Searching for dual AGN in galaxies with double-peaked emission line spectra using radio observations. *Mon. Not. R. Astron. Soc.* **2019**, *484*, 4933–4950. <https://doi.org/10.1093/mnras/stz334>.
83. De Rosa, A.; Vignali, C.; Bogdanović, T.; Capelo, P.R.; Charisi, M.; Dotti, M.; Husemann, B.; Lusso, E.; Mayer, L.; Paragi, Z.; et al. The quest for dual and binary supermassive black holes: A multi-messenger view. *New Astron. Rev.* **2019**, *86*, 101525. <https://doi.org/10.1016/j.newar.2020.101525>.
84. Thorne, K.S.; Braginskii, V.B. Gravitational-wave bursts from the nuclei of distant galaxies and quasars: proposal for detection using Doppler tracking of interplanetary spacecraft. *Astrophys. J.* **1976**, *204*, L1–L6. <https://doi.org/10.1086/182042>.

85. Wang, J.M.; Chen, Y.M.; Hu, C.; Mao, W.M.; Zhang, S.; Bian, W.H. Active Galactic Nuclei with Double-Peaked Narrow Lines: Are they Dual Active Galactic Nuclei? *Astrophys. J.* **2009**, *705*, L76–L80. <https://doi.org/10.1088/0004-637X/705/1/L76>.
86. Smith, K.L.; Shields, G.A.; Bonning, E.W.; McMullen, C.C.; Rosario, D.J.; Salviander, S. A Search for Binary Active Galactic Nuclei: Double-peaked [O III] AGNs in the Sloan Digital Sky Survey. *Astrophys. J.* **2010**, *716*, 866–877. <https://doi.org/10.1088/0004-637X/716/1/866>.
87. Teng, S.H.; Schawinski, K.; Urry, C.M.; Darg, D.W.; Kaviraj, S.; Oh, K.; Bonning, E.W.; Cardamone, C.N.; Keel, W.C.; Lintott, C.J.; et al. Chandra Observations of Galaxy Zoo Mergers: Frequency of Binary Active Nuclei in Massive Mergers. *Astrophys. J.* **2012**, *753*, 165. <https://doi.org/10.1088/0004-637X/753/2/165>.
88. Liu, X.; Shen, Y.; Strauss, M.A. Active Galactic Nucleus Pairs from the Sloan Digital Sky Survey. II. Evidence for Tidally Enhanced Star Formation and Black Hole Accretion. *Astrophys. J.* **2012**, *745*, 94. <https://doi.org/10.1088/0004-637X/745/1/94>.
89. Prabhu, T.P. Indian Astronomical Observatory, Leh-Hanle. *Proc. Indian Natl. Sci. Acad. Part A* **2014**, *80*, 887–912. <https://doi.org/10.16943/ptinsa/2014/v80i4/55174>.
90. Perucho, M.; Martí, J.M. Physical Parameters in the Hot Spots and Jets of Compact Symmetric Objects. *Astrophys. J.* **2002**, *568*, 639–650. <https://doi.org/10.1086/338882>.
91. Bondi, M.; Pérez-Torres, M.A.; Dallacasa, D.; Muxlow, T.W.B. A supernova factory in Mrk 273? *Mon. Not. R. Astron. Soc.* **2005**, *361*, 748–752. <https://doi.org/10.1111/j.1365-2966.2005.09206.x>.
92. Hernández-Ibarra, F.J.; Krongold, Y.; Dultzin, D.; del Olmo, A.; Perea, J.; González, J.; Mendoza-Castrejón, S.; Bitsakis, T. The incidence of nuclear activity in galaxy pairs with different morphologies (E+E), (E+S) and (S+S). *Mon. Not. R. Astron. Soc.* **2016**, *459*, 291–309. <https://doi.org/10.1093/mnras/stw480>.
93. de Bruyn, A.G.; Wilson, A.S. A 1415 MHz Survey of Seyfert and Related Galaxies. *Astron. Astrophys.* **1976**, *53*, 93.
94. Ulvestad, J.S.; Wilson, A.S. Radio structures of Seyfert galaxies. VI. VLA observations of a nearby sample. *Astrophys. J.* **1984**, *285*, 439–452. <https://doi.org/10.1086/162520>.
95. Roy, A.L.; Norris, R.P.; Kesteven, M.J.; Troup, E.R.; Reynolds, J.E. Compact Radio Cores in Seyfert Galaxies. *Astrophys. J.* **1994**, *432*, 496. <https://doi.org/10.1086/174589>.
96. Thean, A.; Pedlar, A.; Kukula, M.J.; Baum, S.A.; O’Dea, C.P. High-resolution radio observations of Seyfert galaxies in the extended 12- μ m sample—II. The properties of compact radio components. *Mon. Not. R. Astron. Soc.* **2001**, *325*, 737–760. <https://doi.org/10.1046/j.1365-8711.2001.04485.x>.
97. Gallimore, J.F.; Axon, D.J.; O’Dea, C.P.; Baum, S.A.; Pedlar, A. A Survey of Kiloparsec-Scale Radio Outflows in Radio-Quiet Active Galactic Nuclei. *Astron. J.* **2006**, *132*, 546–569. <https://doi.org/10.1086/504593>.
98. Jarvis, M.E.; Harrison, C.M.; Thomson, A.P.; Circosta, C.; Mainieri, V.; Alexander, D.M.; Edge, A.C.; Lansbury, G.B.; Molyneux, S.J.; Mullaney, J.R. Prevalence of radio jets associated with galactic outflows and feedback from quasars. *Mon. Not. R. Astron. Soc.* **2019**, *485*, 2710–2730. <https://doi.org/10.1093/mnras/stz556>.
99. Silpa, S.; Kharb, P.; Ho, L.C.; Ishwara-Chandra, C.H.; Jarvis, M.E.; Harrison, C. Probing the origin of low-frequency radio emission in PG quasars with the uGMRT—I. *Mon. Not. R. Astron. Soc.* **2020**, *499*, 5826–5839. <https://doi.org/10.1093/mnras/staa2970>.
100. Kharb, P.; O’Dea, C.P.; Baum, S.A.; Colbert, E.J.M.; Xu, C. A Radio Study of the Seyfert Galaxy Markarian 6: Implications for Seyfert Life Cycles. *Astrophys. J.* **2006**, *652*, 177–188. <https://doi.org/10.1086/507945>.
101. Irwin, J.A.; Schmidt, P.; Damas-Segovia, A.; Beck, R.; English, J.; Heald, G.; Henriksen, R.N.; Krause, M.; Li, J.T.; Rand, R.J.; et al. CHANG-ES—VIII. Uncovering hidden AGN activity in radio polarization. *Mon. Not. R. Astron. Soc.* **2017**, *464*, 1333–1346. <https://doi.org/10.1093/mnras/stw2414>.
102. Rao, V.V.; Kharb, P.; Rubinur, K.; Silpa, S.; Roy, N.; Sebastian, B.; Singh, V.; Baghel, J.; Manna, S.; Ishwara-Chandra, C.H. AGN feedback through multiple jet cycles in the Seyfert galaxy NGC 2639. *Mon. Not. R. Astron. Soc.* **2023**, *524*, 1615–1624. <https://doi.org/10.1093/mnras/stad1901>.
103. Lacerda, E.A.D.; Sánchez, S.F.; Cid Fernandes, R.; López-Cobá, C.; Espinosa-Ponce, C.; Galbany, L. Galaxies hosting an active galactic nucleus: a view from the CALIFA survey. *Mon. Not. R. Astron. Soc.* **2020**, *492*, 3073–3090. <https://doi.org/10.1093/mnras/staa008>.
104. Berrier, J.C.; Davis, B.L.; Kennefick, D.; Kennefick, J.D.; Seigar, M.S.; Barrows, R.S.; Hartley, M.; Shields, D.; Bentz, M.C.; Lacy, C.H.S. Further Evidence for a Supermassive Black Hole Mass-Pitch Angle Relation. *Astrophys. J.* **2013**, *769*, 132. <https://doi.org/10.1088/0004-637X/769/2/132>.
105. Sebastian, B.; Kharb, P.; O’Dea, C.P.; Gallimore, J.F.; Baum, S.A. The discovery of secondary lobes in the Seyfert galaxy NGC 2639. *Mon. Not. R. Astron. Soc.* **2019**, *490*, L26–L31. <https://doi.org/10.1093/mnrasl/slz136>.
106. Sanders, R.H. Seyfert nuclei as short-lived stochastic accretion events. *Astron. Astrophys.* **1984**, *140*, 52–54.
107. Ellison, S.L.; Wong, T.; Sánchez, S.F.; Colombo, D.; Bolatto, A.; Barrera-Ballesteros, J.; García-Benito, R.; Kalinova, V.; Luo, Y.; Rubio, M.; et al. The EDGE-CALIFA survey: central molecular gas depletion in AGN host galaxies—A smoking gun for quenching? *Mon. Not. R. Astron. Soc.* **2021**, *505*, L46–L51. <https://doi.org/10.1093/mnrasl/slab047>.
108. George, K.; Joseph, P.; Mondal, C.; Devaraj, A.; Subramaniam, A.; Stalin, C.S.; Côté, P.; Ghosh, S.K.; Hutchings, J.B.; Mohan, R.; et al. UVIT observations of the star-forming ring in NGC 7252: Evidence of possible AGN feedback suppressing central star formation. *Astron. Astrophys.* **2018**, *613*, L9. <https://doi.org/10.1051/0004-6361/201833232>.

109. George, K.; Poggianti, B.M.; Bellhouse, C.; Radovich, M.; Fritz, J.; Paladino, R.; Bettoni, D.; Jaffé, Y.; Moretti, A.; Gullieuszik, M.; et al. GASP XVIII: star formation quenching due to AGN feedback in the central region of a jellyfish galaxy. *Mon. Not. R. Astron. Soc.* **2019**, *487*, 3102–3111. <https://doi.org/10.1093/mnras/stz1443>.
110. Shin, J.; Woo, J.H.; Chung, A.; Baek, J.; Cho, K.; Kang, D.; Bae, H.J. Positive and Negative Feedback of AGN Outflows in NGC 5728. *Astrophys. J.* **2019**, *881*, 147. <https://doi.org/10.3847/1538-4357/ab2e72>.
111. Joseph, P.; George, K.; Paul, K.T. Active galactic nucleus feedback in NGC 3982. *Astron. Astrophys.* **2022**, *667*, A88. <https://doi.org/10.1051/0004-6361/202243923>.
112. Giroletti, M.; Panessa, F. The Faintest Seyfert Radio Cores Revealed by VLBI. *Astrophys. J.* **2009**, *706*, L260–L264. <https://doi.org/10.1088/0004-637X/706/2/L260>.
113. Jones, S.; McHardy, I.; Moss, D.; Seymour, N.; Breedt, E.; Uttley, P.; Körding, E.; Tudose, V. Radio and X-ray variability in the Seyfert galaxy NGC 4051. *Mon. Not. R. Astron. Soc.* **2011**, *412*, 2641–2652. <https://doi.org/10.1111/j.1365-2966.2010.18105.x>.
114. Riffel, R.A.; Storch-Bergmann, T.; Winge, C.; McGregor, P.J.; Beck, T.; Schmitt, H. Mapping of molecular gas inflow towards the Seyfert nucleus of NGC4051 using Gemini NIFS. *Mon. Not. R. Astron. Soc.* **2008**, *385*, 1129–1142. <https://doi.org/10.1111/j.1365-2966.2008.12936.x>.
115. Lammers, C.; Iyer, K.G.; Ibarra-Medel, H.; Pacifici, C.; Sánchez, S.F.; Tacchella, S.; Woo, J. Active Galactic Nuclei Feedback in SDSS-IV MaNGA: AGNs Have Suppressed Central Star Formation Rates. *Astrophys. J.* **2023**, *953*, 26. <https://doi.org/10.3847/1538-4357/acdd57>.
116. Laing, R.A.; Riley, J.M.; Longair, M.S. Bright radio sources at 178 MHz : flux densities, optical identifications and the cosmological evolution of powerful radio galaxies. *Mon. Not. R. Astron. Soc.* **1983**, *204*, 151–187. <https://doi.org/10.1093/mnras/204.1.151>.
117. Salomé, Q.; Salomé, P.; Combes, F. Jet-induced star formation in 3C 285 and Minkowski’s Object. *Astron. Astrophys.* **2015**, *574*, A34. <https://doi.org/10.1051/0004-6361/201424932>.
118. Spinrad, H.; Djorgovski, S.; Marr, J.; Aguilar, L. A third update of the status of the 3 CR sources: Further new redshifts and new identifications of distant galaxies. *Publ. Astron. Soc. Pac.* **1985**, *97*, 932–961. <https://doi.org/10.1086/131647>.
119. McCarthy, P.J.; Spinrad, H.; van Breugel, W. Emission-Line Imaging of 3CR Radio Galaxies. I. Imaging Data. *Astrophys. J. Suppl. Ser.* **1995**, *99*, 27. <https://doi.org/10.1086/192178>.
120. Best, P.N.; Longair, M.S.; Rottgering, H.J.A. A jet-cloud interaction in 3C 34 at redshift $z=0.69$. *Mon. Not. R. Astron. Soc.* **1997**, *286*, 785–794. <https://doi.org/10.1093/mnras/286.4.785>.
121. van Breugel, W.J.M.; Dey, A. Induced Star Formation in a Radio Lobe of 3C 285? *Astrophys. J.* **1993**, *414*, 563. <https://doi.org/10.1086/173103>.
122. Croft, S.; van Breugel, W.; de Vries, W.; Dopita, M.; Martin, C.; Morganti, R.; Neff, S.; Oosterloo, T.; Schiminovich, D.; Stanford, S.A.; et al. Minkowski’s Object: A Starburst Triggered by a Radio Jet, Revisited. *Astrophys. J.* **2006**, *647*, 1040–1055. <https://doi.org/10.1086/505526>.
123. Lacy, M.; Croft, S.; Fragile, C.; Wood, S.; Nyland, K. ALMA Observations of the Interaction of a Radio Jet with Molecular Gas in Minkowski’s Object. *Astrophys. J.* **2017**, *838*, 146. <https://doi.org/10.3847/1538-4357/aa65d7>.
124. Bolton, J.G.; Stanley, G.J.; Slee, O.B. Positions of Three Discrete Sources of Galactic Radio-Frequency Radiation. *Nature* **1949**, *164*, 101–102. <https://doi.org/10.1038/164101b0>.
125. Israel, F.P. Centaurus A—NGC 5128. *A&A Rev.* **1998**, *8*, 237–278. <https://doi.org/10.1007/s001590050011>.
126. Charmandaris, V.; Combes, F.; van der Hulst, J.M. First detection of molecular gas in the shells of CenA. *Astron. Astrophys.* **2000**, *356*, L1–L4. <https://doi.org/10.48550/arXiv.astro-ph/0003175>.
127. Harris, G.L.H.; Rejkuba, M.; Harris, W.E. *The Distance to NGC 5128 (Centaurus A)*; Cambridge University Press: Cambridge, UK, 2010; Volume 27, pp. 457–462. <https://doi.org/10.1071/AS09061>.
128. Wang, J.; Hammer, F.; Rejkuba, M.; Crnojević, D.; Yang, Y. A recent major merger tale for the closest giant elliptical galaxy Centaurus A. *Mon. Not. R. Astron. Soc.* **2020**, *498*, 2766–2777. <https://doi.org/10.1093/mnras/staa2508>.
129. Junkes, N.; Haynes, R.F.; Harnett, J.I.; Jauncey, D.L. Radio polarization surveys of Centaurus A (NGC 5128). I. The complete radio source at lambda 6.3 cm. *Astron. Astrophys.* **1993**, *269*, 29–38.
130. Wykes, S.; Intema, H.T.; Hardcastle, M.J.; Achterberg, A.; Jones, T.W.; Jerjen, H.; Orrú, E.; Lazarian, A.; Shimwell, T.W.; Wise, M.W.; et al. Filaments in the southern giant lobe of Centaurus A: constraints on nature and origin from modelling and GMRT observations. *Mon. Not. R. Astron. Soc.* **2014**, *442*, 2867–2882. <https://doi.org/10.1093/mnras/stu1033>.
131. McKinley, B.; Tingay, S.J.; Carretti, E.; Ellis, S.; Bland-Hawthorn, J.; Morganti, R.; Line, J.; McDonald, M.; Veilleux, S.; Wahl Olsen, R.; et al. The jet/wind outflow in Centaurus A: a local laboratory for AGN feedback. *Mon. Not. R. Astron. Soc.* **2018**, *474*, 4056–4072. <https://doi.org/10.1093/mnras/stx2890>.
132. McKinley, B.; Tingay, S.J.; Gaspari, M.; Kraft, R.P.; Matherne, C.; Offringa, A.R.; McDonald, M.; Calzadilla, M.S.; Veilleux, S.; Shabala, S.S.; et al. Multi-scale feedback and feeding in the closest radio galaxy Centaurus A. *Nature Astronomy* **2022**, *6*, 109–120. <https://doi.org/10.1038/s41550-021-01553-3>.
133. Neff, S.G.; Eilek, J.A.; Owen, F.N. The Complex North Transition Region of Centaurus A: Radio Structure. *Astrophys. J.* **2015**, *802*, 87. <https://doi.org/10.1088/0004-637X/802/2/87>.
134. Morganti, R.; Killeen, N.E.B.; Ekers, R.D.; Oosterloo, T.A. Centaurus A: multiple outbursts or bursting bubble? *Mon. Not. R. Astron. Soc.* **1999**, *307*, 750–760. <https://doi.org/10.1046/j.1365-8711.1999.02622.x>.

135. Kraft, R.P.; Forman, W.R.; Hardcastle, M.J.; Birkinshaw, M.; Croston, J.H.; Jones, C.; Nulsen, P.E.J.; Worrall, D.M.; Murray, S.S. The Jet Heated X-Ray Filament in the Centaurus A Northern Middle Radio Lobe. *Astrophys. J.* **2009**, *698*, 2036–2047. <https://doi.org/10.1088/0004-637X/698/2/2036>.
136. Neff, S.G.; Eilek, J.A.; Owen, F.N. The Complex North Transition Region of Centaurus A: A Galactic Wind. *Astrophys. J.* **2015**, *802*, 88. <https://doi.org/10.1088/0004-637X/802/2/88>.
137. Rejkuba, M.; Minniti, D.; Silva, D.R.; Bedding, T.R. Stellar populations in NGC 5128 with the VLT: Evidence for recent star formation. *Astron. Astrophys.* **2001**, *379*, 781–797. <https://doi.org/10.1051/0004-6361:20011315>.
138. Rejkuba, M.; Minniti, D.; Courbin, F.; Silva, D.R. Radio-Optical Alignment and Recent Star Formation Associated with Ionized Filaments in the Halo of NGC 5128 (Centaurus A). *Astrophys. J.* **2002**, *564*, 688–695. <https://doi.org/10.1086/324500>.
139. Eilek, J.A. The dynamic age of Centaurus A. *New J. Phys.* **2014**, *16*, 045001. <https://doi.org/10.1088/1367-2630/16/4/045001>.
140. Salomé, Q.; Salomé, P.; Combes, F.; Hamer, S.; Heywood, I. Star formation efficiency along the radio jet in Centaurus A. *Astron. Astrophys.* **2016**, *586*, A45. <https://doi.org/10.1051/0004-6361/201526409>.
141. Oosterloo, T.A.; Morganti, R. Anomalous HI kinematics in Centaurus A: Evidence for jet-induced star formation. *Astron. Astrophys.* **2005**, *429*, 469–475. <https://doi.org/10.1051/0004-6361:20041379>.
142. Joseph, P.; Sreekumar, P.; Stalin, C.S.; Paul, K.T.; Mondal, C.; George, K.; Mathew, B. UVIT view of Centaurus A: a detailed study on positive AGN feedback. *Mon. Not. R. Astron. Soc.* **2022**, *516*, 2300–2313. <https://doi.org/10.1093/mnras/stac2388>.
143. Leitherer, C.; Schaerer, D.; Goldader, J.D.; Delgado, R.M.G.; Robert, C.; Kune, D.F.; de Mello, D.F.; Devost, D.; Heckman, T.M. Starburst99: Synthesis Models for Galaxies with Active Star Formation. *Astrophys. J. Suppl. Ser.* **1999**, *123*, 3–40. <https://doi.org/10.1086/313233>.
144. Chambers, K.C.; Miley, G.K.; van Breugel, W.J.M. 4C 41.17: A Radio Galaxy at a Redshift of 3.8. *Astrophys. J.* **1990**, *363*, 21. <https://doi.org/10.1086/169316>.
145. Nesvadba, N.P.H.; Bicknell, G.V.; Mukherjee, D.; Wagner, A.Y. Gas, dust, and star formation in the positive AGN feedback candidate 4C 41.17 at $z = 3.8$. *Astron. Astrophys.* **2020**, *639*, L13. <https://doi.org/10.1051/0004-6361/202038269>.
146. Ignesti, A.; Brienza, M.; Vulcani, B.; Poggianti, B.M.; Marasco, A.; Smith, R.; Hardcastle, M.J.; Botteon, A.; Roberts, I.D.; Fritz, J.; et al. On the Encounter between the GASP Galaxy JO36 and the Radio Plume of GIN 049. *Astrophys. J.* **2023**, *956*, 122. <https://doi.org/10.3847/1538-4357/acf70f>.
147. Subramaniam, A. An overview of the proposed Indian spectroscopic and imaging space telescope. *J. Astrophys. Astron.* **2022**, *43*, 80. <https://doi.org/10.1007/s12036-022-09870-3>.
148. Kulkarni, S.R.; Harrison, F.A.; Grefenstette, B.W.; Earnshaw, H.P.; Andreoni, I.; Berg, D.A.; Bloom, J.S.; Cenko, S.B.; Chornock, R.; Christiansen, J.L.; et al. Science with the Ultraviolet Explorer (UVEX). *arXiv* **2021**, arXiv:2111.15608. <https://doi.org/10.48550/arXiv.2111.15608>.

Disclaimer/Publisher’s Note: The statements, opinions and data contained in all publications are solely those of the individual author(s) and contributor(s) and not of MDPI and/or the editor(s). MDPI and/or the editor(s) disclaim responsibility for any injury to people or property resulting from any ideas, methods, instructions or products referred to in the content.